Accepted Manuscript

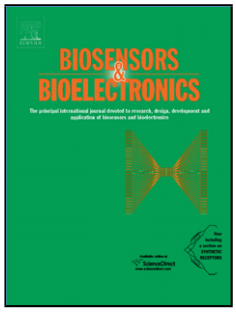

Title: Improved bacteria detection by coupling magneto-immunocapture and amperometry at flow-channel microband electrodes

Authors: Olivier Laczka, José-María Maesa, Neus Godino, Javier del Campo, Mikkel Fougt-Hansen, Jorg P. Kutter, Detlef Snakenborg, Francesc-Xavier Muñoz-Pascual, Eva Baldrich

PII: S0956-5663(11)00106-0
DOI: doi:10.1016/j.bios.2011.02.019
Reference: BIOS 4363

To appear in: *Biosensors and Bioelectronics*

Received date: 10-11-2010
Revised date: 13-1-2011
Accepted date: 12-2-2011

Please cite this article as: Laczka, O., Maesa, J.-M., Godino, N., del Campo, J., Fougt-Hansen, M., Kutter, J.P., Snakenborg, D., Muñoz-Pascual, F.-X., Baldrich, E., Improved bacteria detection by coupling magneto-immunocapture and amperometry at flow-channel microband electrodes, *Biosensors and Bioelectronics* (2010), doi:10.1016/j.bios.2011.02.019

Improved bacteria detection by coupling magneto-immunocapture and amperometry at flow-channel microband electrodes

Olivier Laczka[1], José-María Maesa[1], Neus Godino[1], Javier del Campo[1], Mikkel Fougt-Hansen[2], Jorg P. Kutter[2*], Detlef Snakenborg[2], Francesc-Xavier Muñoz-Pascual[1], Eva Baldrich[1**]

[1] Institut de Microelectrònica de Barcelona (IMB-CNM), CSIC, Esfera UAB Campus Universitat Autònoma de Barcelona, 08193 – Bellaterra (Barcelona), Spain

[2] Department of Micro- and Nanotechnology, Technical University of Denmark, DTU Nanotech, Building 345 East, DK-2800 Kongens, Lyngby, Denmark

Corresponding authors:

* Jörg Kutter
Department of Micro- and Nanotechnology, Technical University of Denmark, DTU Nanotech, Building 345 East, DK-2800 Kongens, Lyngby, Denmark
E-mail: joerg.kutter@nanotech.dtu.dk
Telephone: (+45) 4525 5785
Fax number: (+45) 45887762

** Eva Baldrich
Address: Institut de Microelectrònica de Barcelona (IMB-CNM, CSIC). Campus Universitat Autònoma de Barcelona. Barcelona 08193 (Spain)
E-mail: eva.baldrich@imb-cnm.csic.es
Telephone: (+34) 93 5947700 (ext 2405)
Fax number: (+34) 93 58014 96

ABSTRACT

This paper describes the first immunosensing system reported for the detection of bacteria combining immunomagnetic capture and amperometric detection in a one-step sandwich format, and in a microfluidic environment. Detection is based on the electrochemical monitoring of the activity of horseradish peroxidase (HRP), an enzyme label, through its catalysis of hydrogen peroxide (H_2O_2) in the presence of the mediator hydroquinone (HQ). The enzymatic reaction takes place in an incubation micro-chamber where the magnetic particles (MP) are confined, upstream from the working electrode. The enzyme product is then pumped along a microchannel, where it is amperometrically detected by a set of microelectrodes. This design avoids direct contact of the biocomponents with the electrode, which lowers the risk of electrode fouling. The whole assay can be completed in 1 hour. The experiments performed with *E. coli* evidenced a linear response for concentrations ranging 10^2-10^8 cell ml^{-1}, with a limit of detection of 55 cells ml^{-1} in PBS, without pre-enrichment steps. Furthermore, 100 cells ml^{-1} could be detected in milk, and with negligible interference by non-target bacteria such as *Pseudomonas*.

Keywords

Amperometric immunosensor; bacteria detection; immunomagnetic capture; microfluidic system; electrochemical detection.

1. **Introduction**

Bacteria detection is a permanent concern in a wide range of fields, including the food, pharmaceutical and water treatment industries, in which fast detection is critical to prevent microbial outbreaks. Milk is one of the media where foodborne pathogens thrive, and in the past it has been the origin of diseases such as tuberculosis, brucellosis, diphtheria, and scarlet fever (Vasavada 1988; Baylis 2009). The risk of outbreaks has been significantly reduced thanks to the modern production practices, including sanitary control of the herds, appropriate handling, cooling and storage conditions, and specially pasteurization. Nevertheless, contaminated milk can reach the consumer in cases of incomplete pasteurization, innadequate storing, and/or post-processing contamination. For example, an outbreak detected in Austria in June 2007 afected 40 children who had consumed pasteurized milk products (Schmid et al., 2009). And milk or milk products were suspected to cause 177 outbreaks in France between 1988-1997 (De Buyser et al., 2001). Accordingly, there is a strong necessity for developing sensitive and accurate biosensors and portable lab-on-a-chip devices capable of rapid and versatile analyses (G. Ocvirk et al., 1998; E. T. Lagally et al., 2004; N. Beyor et al., 2008). *Escherichia coli* is the model microorganism most widely used in biosensing development. This is due to its ubiquity, and because *E. coli* is responsible for numerous water- and food-transmitted infections (P. M. Griffin and Tauxe 1991; F. Perez et al., 2001; J. H. Thomas et al., 2003; H. S. Hussein and Bollinger 2005).

Immunofunctionalised magnetic particles (MP) and immunomagnetic separation (IMS) have been proposed as new and versatile tools for biosensing (Hsing et al., 2007; Jaffrezic-Renault et al., 2007). Using MP allows fast, simple, and specific pre-concentration of target bacteria from relatively large and dilute sample volumes, as well as physical separation from non-target components occurring in complex sample matrices. In addition, MP provide large surface areas which, in combination with rotation with the sample, generate enhanced target-antibody kinetics, shorter assay times, and improved limits of detection (LOD) (Hsing et al., 2007; Jaffrezic-Renault et al., 2007). Bacteria detection on MP has been usually based on classical sandwich assay formats, in which bacterial IMS is followed by detection using a labeled-antibody (Ab). Mainly coupled to colorimetric, fluorescent or

chemiluminiscent detection, those assays had reported LODs of 10^3-10^6 cell ml^{-1} within assay times of 1-2 h, and could be carried out even in real sample matrices such as water or milk (Nakamura et al., 1993; Bruno et al., 1996; Yu 1998; Yu et al., 2000; Tu et al., 2001; Tu et al., 2003; Gehring et al., 2006; Baldrich and Muñoz 2008).

MP offer an additional advantage: the possibility to integrate IMS and microfluidics technology (Gijs et al., 2010). Microfluidic systems enable the analysis of small sample volumes, as well as the utilization and disposal of minute amounts of reagents. The integration of several assay steps in-chip facilitates and accelerates manipulation. In addition, operation under flow conditions improves immunocapture, enzymatic reactions and electrochemical detection by minimising the limitation of mass transport, contributing to reduce assay time. At least one work reports on a flow-through immunomagnetic separator designed to capture bacteria from large volume samples (>50 ml) (Rotariu et al., 2005) and an increasing number of publications describe the automation of MP manipulation, recovery, and/or detection (Herrmann et al., 2008; Hervas et al., 2009; Peyman et al., 2009; Yoon et al., 2009; Berti et al., 2009 ; Johansson et al., 2010). However, only a few cases describe the application to immunocapture and detection of whole bacterial cells (Chandler et al., 2001; Straub et al., 2005; Qiu et al., 2009; Ramadan et al., 2010).

For example, Qiu employed a U-shaped microchannel with two magnets to entrap immunofunctionalised MP (Qiu et al., 2009), which granted specific capture of the target microorganisms. MP were then eluted and fluorescent detection of bacterial ATP was performed out of the chip. Ramadan reported an original device integrating a serpentine channel with rows of rotating magnets (Ramadan et al., 2010). Following MP injection, magnet rotation induced their subsequent entrapment and release. As a consequence, MP moved along the channel while being washed, and provided recovery efficiencies of about 83-90% for *Giardia* and *Cryptosporidium* from tap water samples, and of about 18-36% in spiked secondary effluent water samples. Nonetheless, MP immunocapture, bacteria staining, and detection using a fluorescence microscope were performed outside the chip. Chadler, on the other hand, used a Teflon tube (19.1 mm long x 2.1 mm wide) filled with Ni foam to retain immunofunctionalised MP (Chandler et al., 2001). PBS or poultry carcass rinse samples, spiked with *E. coli*, were perfused over the MP in a back-and-forth stepped-flow regime, which promoted mixing and extended contact time. After MP

release, *E. coli* was detected by Polymerase Chain Reaction (PCR) down to an initial concentration of 10^3 cell ml^{-1}. The latter integration of a flow-through PCR reaction chamber, followed by elution and off-line microarray hybridisation and fluorescent detection, provided identification of 10 *E. coli* cells spiked in 1 ml of water in the absence of interferent bacteria (Straub et al., 2005).

Here we apply a simple, reusable and portable electroanalytical microchannel flow cell to detection of pathogen bacteria. First, a classical two-step sandwich ELISA is formatted into a one-step sandwich immunomagnetic assay. Thus assay time is shortened and sample manipulation is simplified without negatively affecting detectability. MP are then analysed using a flow cell (Figure 1), which encloses an incubation microchamber, a microfluidic channel, and a silicon chip containing a set of electrodes (Godino et al., 2010). While MP are magnetically retained in the microchamber, the enzyme product flows and is chronoamperometrically detected at the gold microband electrode located downstream. Capturing the MP upstream from the microelectrodes presents an innovation over the general trend to capturing them directly over the electrodes (Choi et al., 2002; Do and Ahn 2008): it provides better control over the mass transport conditions, which leads to higher currents, and protects the electrode surface from fouling and passivation.

Under these conditions, the specific detection of *E. coli* was successful in a concentration range between 10^2-10^8 cell ml^{-1} with an LOD of 55 cell ml^{-1} and little interference by non-target *Pseudomonas*. Furthermore, 100 cell ml^{-1} of *E. coli* were consistently detected in 10% milk. These results demonstrate the value of this combination of immunomagnetic capture, electrochemical detection, and microfluidic technology for the detection of pathogen bacteria even in complex sample matrices.

2. Materials and methods

2.1. Chemical reagents and biocomponents

Phosphate Buffered Saline 0.01 M tablets (PBS), streptavidin-coated Dynabeads (M-270, 2.8 µm diameter), and biotinylated horseradish peroxidase (HRP) were obtained from Invitrogen (Barcelona, Spain). Biotinylated and HRP-labelled anti-*E. coli* polyclonal Ab were respectively purchased from AbCam (Cambridge, UK) and US Biological (Massachusetts, USA). Hydroquinone (HQ), 3,3',5,5'-

Tetramethylbenzidine liquid substrate system (TMB), KCl, KNO_3, $K_4Fe(CN)_6.3H_2O$, $K_3Fe(CN)_6$, *p*-benzoquinone (BQ) and hydrogen peroxide (30%) were purchased from Sigma (Barcelona, Spain).

2.2. Preparation and handling of bacteria

Escherichia coli K12 and *Pseudomonas putida* KT 2442 were obtained from the American Type Cells Collection. Bacteria were grown overnight in Luria-Bertani (LB) liquid medium at 37ºC. The cultures were serially diluted and agar plated to obtain the viable counts (colony-forming units [CFU]). The cultures were then aliquoted into eppendorf tubes and centrifuged for 10 minutes at 12000 rpm. The supernatants were discarded, and ready-to-use pellets were stored at -20 ºC until needed (Baldrich et al., 2008). Before reconstitution, frozen pellets were temperated at 4 ºC for 10 minutes. The pellets were re-suspended in 50 µl of the desired solution and, after agitation and complete re-suspension, the volume was completed to 1 ml.

2.3. Functionalisation of MP

Two types of customized MP, enzyme-modified MP and anti-*E. coli* MP, were prepared by modifying streptavidin-coated Dynabeads with biotinylated HRP and biotinylated anti-*E. coli* polyclonal Ab respectively (approximately 3.3 µg of HRP or 1 µg of Ab per 7 x 10^6 MP). Briefly, protein and MP were agitated for 30 min at room temperature, washed with PBS containing 0.1% (v/v) Tween 20 (PBS-T), treated with biotin excess for 5 min in order to block the remaining biotin-binding sites, and stored until used at 4ºC (approximately 7×10^8 MP ml^{-1}) in PBS containing 0.1% bovine serum albumin (BSA).

2.4. Sandwich immunoassay on MP

Immediately prior to assay performance, the anti-*E. coli* MP were completely resuspended by vortexing for 1–2 minutes. Bacteria were serially diluted in PBS containing 0.01% Tween 20. Approximately 7×10^6 MP and 4 µg of HRP-labelled anti-*E.coli* Ab were added per ml of sample. The samples were then rotated for 40 minutes at room temperature, concentrated using a magnet (BILATEST; Bilatec AG; Stuttgart, Germany), and washed twice with PBS-T for 5 minutes in continuous

rotation.

2.5 Spectrophotometric measurements

For the colorimetric detection of the sandwich immunoassay, MP were resuspended in 15 µl PBS-T, transferred to a microtitter plate, and TMB was added (100 µl per well). After 25 minutes, the enzymatic reaction was stopped with 100 µl H_2SO_4 0.1 M per well and absorbance was measured at 450 nm.

2.6. Electrochemical measurements using the microfluidic system

The HRP substrate/mediator solution contained 1 mM H_2O_2 and 1 mM HQ in deoxygenated PBS (pH 7). The composition and pH of this substrate solution was optimised experimentally (data not shown).

MP were resuspended in 400 µl PBS pH7 and 200 µl were injected in the microfluidic cell at 50 µl min^{-1}. The cell was then filled with 100 µl of substrate/mediator solution, the flow rate was stopped and the enzyme was allowed to react with the substrate for 5 minutes. Finally, the substrate flow was resumed at 10 µl min^{-1} and the current was measured at -0.35 V using a CHI700C bipotentiostat (CH Instruments, Texas, USA). The whole system was extensively washed between measurements by flowing PBS in order to avoid sample cross-contamination.

The microband gold electrodes were fabricated using standard photolithographic techniques. Briefly, a 50-nm adhesion layer of Ti and a 200 nm layer of Au were sequentially deposited by e-beam evaporation, and the electrodes were defined by lift-off. Each device consisted of three bands 500 µm wide and one band 1 mm wide, all parallel and separated from each other by 100 µm gaps. The wider band was used as auxiliary electrode. Although the remaining three bands could be indistinctly used as working or pseudo-reference electrode, the upstream-most microband was used as the pseudo-reference to avoid potential shifts during the measurements.

The microfluidic system consisted of three components (Figure 1). The bottom (1), made of polycarbonate (PC), contained a pocket for housing the chip and two magnets to promote confinement of the MP upstream from the electrode. The MP could be subsequently released by sliding a metal piece between the magnets and the chip, which allowed performing consecutive experiments. The top closure (2), fabricated in polymethylmethacrylate (PMMA), featured the fluidic interconnections

and a pocket for a polydimethylsiloxane (PDMS) gasket. The solutions were fed in and out through blunt syringe needles and spring-loaded pins provided electrical connection to the chip. Finally, a PDMS gasket, clamped between 1 and 2, provided water-tight sealing and contained all the microfluidic features of the system. These consisted of a cavity 2 mm wide, 150 µm high and 5 mm long that sat directly above the magnets, exiting to a channel 500 µm wide and of the same height that leads the solution out of the system after passing over the electrodes. The flow was controlled using a syringe pump, NE1000 (New Era Pump Systems, NY).

2.7. Data analysis

The results presented come from no less than 3 replicates and the error bars correspond to the standard deviation of the measurements. The limits of detection (LOD) were calculated from the average of the blanks (assay carried out in the absence of target bacteria) plus three times their standard deviation.

3. Results and discussion

3.1. Optimisation of the one-step sandwich immunoassay on MP

The optimisation of the sandwich immunoassay on MP was carried out via colorimetric detection using TMB as the HRP mediator. With this aim, anti-*E. coli* MP were produced and were used to capture increasing concentrations of *E. coli*. It followed washing, incubation with anti-*E. coli* HRP-Ab, and addition of enzyme substrate. After assaying different biocomponent concentrations and incubation times, optimal results were obtained for 30-minute immunocaptures with 7 x 10^6 MP ml^{-1}, followed by incubation with 4 µg HRP-Ab for 60 min, and two washes of 5 min in rotation between each two steps. Under these conditions, the assay detected *E. coli* in a concentration range from 10^4 to 10^8 cell ml^{-1} with an LOD of 3 x 10^3 cell ml^{-1} (Figure 2a). This is two orders of magnitude below the LOD reported for the same Ab set used in a classical ELISA on microtitter plates (Laczka et al., 2008).

Assay shortening was next attempted by combining bacteria immunocapture and binding by HRP-Ab in a single assay step. Hence, anti-*E. coli* MP and HRP-Ab were simultaneously added to samples, which were then rotated at room temperature for

20-60 minutes. The best results were obtained for a 40-minute incubation time in the presence of 4 µg HRP-Ab (Figure 2b). Longer incubations induced higher signals, but also higher level of Ab-HRP non-specific adsorption and background noise and worse assay LOD. Even if the one-step assay generated lower signals than the two-step format, the results were comparable in terms of LOD (5 x 10^3 cells ml^{-1}), and it was shorter and easier to perform (Figure 2a).

Figure 2c shows the specificity of the one-step sandwich assay, which was determined by comparison between the signals obtained for *E. coli* (due to specific immunocapture) and those obtained for the negative-control bacteria *Pseudomonas putida* (caused by non-specific adsorption). The assay showed low signals over the entire *Pseudomonas* concentration range.

3.2. Electrochemical characterization of the microchannel flow cell

Despite its electroactivity (Volpe et al., 1998; Díaz-González et al., 2005; Fanjul-Bolado et al., 2005; Baldrich et al., 2009), TMB could not be used in our microfluidic system because the reaction product precipitated over the MP, which hampered electrochemical detection downstream. Instead, we used hydroquinone/benzoquinone (HQ/BQ) (Elyacoubia et al., 2006; Ji et al., 2007).

In this system, HRP catalyses the reduction of hydrogen peroxide (H_2O_2) coupled to the oxidation of HQ into BQ (Eq. 1). BQ is then electrochemically reduced back into HQ at the electrode surface (Eq. 2), generating a reduction wave around -0.35 V vs. Au.

$$H_2O_2 + HQ \xrightarrow{HRP} 2H_2O + BQ \quad (1)$$

$$BQ + 2H^+ + 2e^- \longrightarrow HQ \quad (2)$$

In the presence of HRP, production of BQ should be directly related to the amount of enzyme. To verify this, streptavidin-coated MP were used to capture increasing quantities of biotynilated HRP and the HRP-MP were injected into the microfluidic cell. The MP were trapped by the magnets on top of the chip, while the solution flowed through. Physical obstruction of either tubes or channel by MP aggregates was never observed. The cell was then filled with substrate/mediator solution and

the flow stopped for 5 minutes to allow the enzyme reaction to proceed. Flow was restored and the chronoamperometric measurement started. After each measurement, an iron slab was slid between the magnets and the microchannel to block the magnetic field, and the whole system was extensively washed by flowing PBS. This released the MP, washed away all the enzyme, and prevented crossed contamination between samples.

Figure 3a shows the signals obtained for the different HRP concentrations. As soon as the flow is restored, the BQ produced over 5 minutes at the HRP-MP is carried towards the electrodes. Here, BQ is reduced, resulting in a marked reduction peak at the beginning of the measurement. It follows current stabilisation, which is an indicator of the actual enzymatic reaction rate. Both the height and width of the initial reduction peak and the steady-state current intensity subsequently registered were proportional to the quantity of HRP captured on the surface of the HRP-MP.

The study of peaks generated as a result of enzyme product accumulation during the transition between flow rates reportedly provided increased sensitivity for β-galactosidase detection (Godino et al., 2010). In the HRP-HQ system, however, wider peaks and lower initial currents (t=0) were registered for the highest concentrations of HRP tested, which indicated that part of the BQ produced diffused towards the electrodes during the incubation step. Hence, the initial reduction peak was only informative for the study of low-to-medium HRP concentrations. This was attributed to the different kinetics of the two enzymes but was not studied further. On the contrary, the current values registered at the steady state were reproducible over a wide range of HRP concentrations (Figure 3b) and provided an LOD of 1pg ml^{-1} of HRP.

3.3. Detection of *E. coli* using the one-step immunoassay at the microchannel flow cell

Next, different concentrations of *E. coli* were assayed using the one-step immunoassay coupled to amperometric detection at the flow cell. Performing immunomagnetic capture and washing outside the detector chip provided optimal mixing and target capture ratios and minimal contact of free biocomponents with the microchannel. Only half of each sample was injected into the flow cell (3.5×10^6 MP) because injecting more beads produced uneven distribution on surface and

presumably packaging into multi-layers, which affected the reproducibility of the assay. Figure 4 shows the currents registered at the steady-state after 250 seconds of measurement. *E. coli* could be detected in a concentration range of 10^2-10^8 cells ml^{-1}, with an LOD of 55 cells ml^{-1}. Simultaneously, the negative controls with no bacteria or with non-target *Pseudomonas putida* evidenced very low levels of both non-specific adsorption and antibody crossbinding. For example, the signals obtained for 10^8 cells ml^{-1} *P. putida* were always below the signals generated by the capture of 10^2 cells ml^{-1} of target *E. coli*. The whole assay, including 40 min of immunoassay, 2 washes of 5 min each, injection into the microfluidic system and enzyme monitoring, took about 1 h. Hence, the present assay has an LOD 2 and 4 orders of magnitude below that of the colorimetric ELISA performed on MP and microtitter plates respectively, and is 30 minutes shorter.

3.4. Detection in milk samples

In order to assess the performance of the reported method in a more complex matrix such as milk, 10^2 *E. coli* cells were inoculated in either milk (dissolved to 10% with PBS) or PBS and were processed as described before. The results are summarised in Figure 5. As before, immunocapture and washing were followed by magnetic capture of the MP on top of the chip and cell filling with substrate/mediator solution. In this case, the flow was stopped to allow the enzyme reaction to proceed but the measument started immediately in order to provide accurate background signals. After 5 minutes of incubation, flow was restored. Again, BQ produced over 5 minutes at the MP moved towards the electrodes and was reduced. This resulted in a marked reduction peak, which was followed by current stabilisation. The changes in signal measured in the negative controls were mainly atributed to non-specific adsorption of HRP-Ab on the MP, also detectable in the colorimetric assay.

Despite being subject to larger errors, in the presence of low concentrations of HRP the initial current peaks gave higher relative signals than the subsequent steady state currents and were proportional to the amount of captured bacteria. The values of the current peaks obtained for the MP incubated in PBS were more than twice those registered for the MP incubated in 10% milk (on average 26.8 and 12.1 nA respectively). Nevertheless, the signal to noise ratio (signal registered for the

bacteria-containing sample divided by background signal recorded for the corresponding negative control) were of the same order in both PBS and milk samples (around 1.6 and 1.7 in that order). Because the electrochemical detection is carried out similarly in both cases, the differences rather evidence changes in immunocapture efficiency. In this respect, it is known that immunocapture is negatively affected in media of increased viscosity, where the ligand diffusion coefficient and the Ab/target binding rate are reduced (Baldrich et al., 2008). At the same time, the background signals were lower in milk, presumably caused by lower levels of HPR-Ab non-specific adsorption in a richer sample matrix. Regardless of this, peak heights were higher in milk samples containing bacteria than in the blanks, demonstrating that as little as 100 *E. coli* cells ml^{-1} can be detected in this sample matrix.

The minimal number of viable *E. coli* bacteria that can produce disease, known as the infectious dose, fluctuates between 10^4-10^8 cells, depending on the strain and the individual (Kothary and Babu 2001). In the specific case of verotoxigenic *E. coli* O157:H7, the infectious dose is lower and just 700 bacteria seem able to cause illness (CDC et al., 2004). Nevertheless, current safety regulations require that bacterial presence at the end of the elaboration process of milk derivatives is low enough to guarantee that microorganism can not growth above hazardous levels over storing or post-processing. As an example, the European Union considers innacceptable titters of *Enterobacteriaceae* above 10 cell ml^{-1} for pasteurized milk, and *E. coli* presence over 100 cell ml^{-1} for milk that has undergone a lower heat treatment than pasteurisation (EU 2005; EU 2010). The described combination of a one-step sandwich immunoassay, MP pre-concentration, and microfluidic electrochemical detection allows fast, specific, and sensitive detection of bacteria even in relatively complex sample matrices. Nevertheless, for the application at industrial environments, where the strict requirements of the health authorities have to be met, additional sample pre-concentration and/or pre-enrichment strategies should be implemented.

4. Conclusions

We have developed a novel electrochemical immunosensing assay for bacterial detection that combines a one-step sandwich immunoassay, MP target pre-

concentration, microfluidic technology, and amperometric detection of the label enzyme. The incorporation on a one-step immunoassay contributes to shorten the analysis compared to classical two-step sandwich assays without compromising detectability. Magnetic pre-concentration makes it possible the study of relatively complex sample matrices. The integration of microfluidic technology provides versatility and improved sensitivity to the electrochemical detection. Finally, the unique design of the chips and flow cell define two connected but independent spaces, where the enzymatic and electrochemical reactions take place respectively. This characteristic prevents the physical coverage and/or passivation of the working electrode by MP or by any biocomponents present in the samples and ensures optimal electrode performance.

The results showed that the reported assay detected *E. coli* in a concentration range between 10^2-10^8 cell ml^{-1} with an LOD of 55 cell ml^{-1} and little interference by significantly higher concentrations of non-target *Pseudomonas*. The whole assay takes about 1 hour, including immunoassay, magnetic pre-concentration, washes and electrochemical detection. Hence this system provides a significant improvement in terms of limit of detection and assay time compared to classical ELISA detection. Furthermore, pre-capture of the bacteria within a more complex matrix such as milk was also successful which suggests its potential applicability to the food industry, pharmaceutical, and medical fields, provided that pre-concentration and/or pre-enrichment strategies are implemented.

Acknowledgements

This work was funded by the Spanish Ministry of Science and Innovation (MICINN) through project grant CTQ2009-08595 (MICROPLATE). JdC acknowledges a Ramón y Cajal Fellowship from MICINN.

References

Baldrich, E., del Campo, F.J., Munoz, F.X., 2009. Biosens. Bioelectron. 25(4), 920-926.
Baldrich, E., Muñoz, F.X., 2008. Analyst 133, 1009-1012.
Baldrich, E., Vigues, N., Mas, J., Munoz, F.X., 2008. Analytical Biochemistry 383(1), 68-75.

Baylis, C.L., 2009. Int. J. Dairy Technol. 62(3), 293-307.
Berti, F., Laschia, S., Palchetti, I., Rossier, J.S., Reymond, F., Mascinia, M., Marrazza, G., 2009 Talanta 77, 971-978.
Bruno, J.G., Yu, H., Kilian, J.P., Moore, A.A., 1996. Journal of Molecular Recognition 9(5-6), 474-479.
CDC, Centers for Disease Control, American Medical Association, American Nurses Association, American Nurses Foundation, Center for Food Safety & Applied Nutrition, Food & Drug Administration, Food Safety Inspection Service, and US Agriculture Department (2004). Diagnosis and management of foodborne illnesses: a primer for physicians and other health care professionals. MMWR Recomm Rep. 53**:** 1-33.
Chandler, D.P., Brown, J., Call, D.R., Wunschel, S., Grate, J.W., Holman, D.A., Olson, L., Stottlemyre, M.S., Bruckner-Lea, C.J., 2001. Int. J. Food Microbiol. 70(1-2), 143-154.
Choi, J.W., Oh, K.W., Thomas, J.H., Heineman, W.R., Halsall, h.B., Helmicki, A.J., Henderson, H.T., Ahn, C.H., 2002. Lab Chip 2, 27-30.
De Buyser, M.L., Dufour, B., Maire, M., Lafarge, V., 2001. Int. J. Food Microbiol. 67(1-2), 1-17.
Díaz-González, M., González-García, M.B., Costa-García, A., 2005. Electroanal. 17(21), 1901 – 1918.
Do, J., Ahn, C.H., 2008. Lab Chip 8, 542-549.
E. T. Lagally, J. R. Scherer, R. G. Blazej, N. M. Toriello, B. A. Diep, M. Ramchandani, G. F. Sensabaugh, L. W. Riley, Mathies, R.A., 2004. Anal. Chem. 76, 3162-3170.
Elyacoubia, A., Zayeda, S.I.M., Blankert, B., Kauffmann, J.-M., 2006. Electroanal. 18(4), 345-350.
EU, 2005. EC 2073/2005, Official Journal of the European Union L 338, 1-26.
EU, 2010. EC 365/2010, Official Journal of the European Union L 107, 9-11.
F. Perez, I. Tryland, M. Mascini, Fiksdal, L., 2001. Anal. Chim. Acta. 2, 149-154.
Fanjul-Bolado, P., González-García, M.B., Costa-García, A., 2005. Anal. Bioanal. Chem. 382, 297–302.
G. Ocvirk, T. Tang, Harrison, D.J., 1998. Analyst 123, 1429.
Gehring, A.G., Irwin, P.L., Reed, S.A., Tu, S.-I., 2006. J. Rap. Meth. Autom. Microbiol. 14, 349-361.
Gijs, M.A.M., Lacharme, F., Lehmann, U., 2010. Chem. Rev. 110, 1518–1563.
Godino, N., Snakenborg, D., Kutter, J.P., Emnéus, J., Hansen, M.F., Muñoz, F.X., del Campo, F.J., 2010. Microfluid Nanofluid 8, 393–402.
H. S. Hussein, Bollinger, L.M., 2005. J. Food Prot. 68, 2224-2241.
Herrmann, M., Veres, T., Tabrizian, M., 2008. Anal. Chem. 80, 5160-5167
Hervas, M., Lopez, M.A., Escarpa, A., 2009. Analyst 134(12), 2405-2411.
Hsing, I.M., Xu, Y., Zhao, W.T., 2007. Electroanalysis 19(7-8), 755-768.
J. H. Thomas, N. J. Ronkainen-Matsuno, S. Farell, H. B. Halsall, Heineman, W.R., 2003. Microchem. 74, 267-276.
Jaffrezic-Renault, N., Martelet, C., Chevolot, Y., Cloarec, J.P., 2007. Sensors 7(4), 589-614.
Ji, X., Banks, C.E., Silvester, D.S., Wain, A.J., Compton, R.G., 2007. J. Phys. Chem. C 111, 1496-1504
Johansson, L., Gunnarsson, K., Bijelovic, S., Eriksson, K., Surpi, A., Gothelid, E., Svedlindh, P., Oscarsson, S., 2010. Lab on a Chip 10(5), 654-661.
Kothary, M.H., Babu, U.S., 2001. J. Food Saf. 21(1), 49-73.
Laczka, O., Baldrich, E., del Campo, F.J., Muñoz , F.X., 2008. Anal. Bioanal. Chem. 391, 2825–2835.
N. Beyor, T. S. Seo, P. Liu, Mathies, R.A., 2008. Microdevices 10, 909-917.
Nakamura, N., Burgess, J.G., Yagiuda, K., Kudo, S., Sakaguchi, T., Matsunaga, T., 1993. Anal. Chem. 65(15), 2036-2039.
P. M. Griffin, Tauxe, R.V., 1991. Epidemiol. Rev 13, 60-98.
Peyman, S.A., Iles, A., Pamme, N., 2009. Lab on a Chip 9(21), 3110-3117.
Qiu, J.M., Zhou, Y., Chen, H., Lin, J.M., 2009. Talanta 79(3), 787-795.

Ramadan, Q., Christophe, L., Teo, W., ShuJun, L., Hua, F.H., 2010. Anal. Chim. Acta 673(1), 101-108.
Rotariu, O., Ogden, I.D., MacRae, M., Badescu, V., Strachan, N.J.C.J., 2005. J. Magn. Magn. Mat. 293, 589.
Schmid, D., Fretz, R., Winter, P., Mann, M., Hoger, G., Stoger, A., Ruppitsch, W., Ladstatter, J., Mayer, N., de Martin, A., Allerberger, F., 2009. Wien. Klin. Wochen. 121(3-4), 125-131.
Straub, T.M., Dockendorff, B.P., Quinonez-Diaz, M.D., Valdez, C.O., Shutthanandan, J.I., Tarasevich, B.J., Grate, J.W., Bruckner-Lea, C.J., 2005. J. Microbiol. Methods 62(3), 303-316.
Tu, S.-I., Patterson, D., Briggs, C., Irwin, P., Yu, L., 2001. J. Indus. Microbiol. Biotechnol. 26, 345-349.
Tu, S.I., Golden, M., Fett, W.F., Gehring, A., Irwin, P., 2003. J. Food Saf. 23(2), 75-89.
Vasavada, P.C., 1988. J. Dairy Sci. 71(10), 2809-2816.
Volpe, G., Compagnone, D., Draisci, R., Palleschi, G., 1998. Analyst 123, 1303–1307.
Yoon, D.H., Ha, J.B., Bahk, Y.K., Arakawa, T., Shoji, S., Go, J.S., 2009. Lab on a Chip 9(1), 87-90.
Yu, H., 1998. J. Immunol. Meth. 218, 1-8.
Yu, H., Raymonda, J.M., McMahon, T.M., Campagnari, A.A., 2000. Biosens. Bioelectron. 14, 829.

Figure legends

Figure 1. Scheme of the microfluidic system, which consists of three components. The bottom contains pockets to hold the chip and two magnets that promote MP confinement upstream from the electrode. The top closure features the fluidic interconnections and a pocket for the PDMS gasket. This gasket provides water-tight sealing and contains all the microfluidic features: a cavity 2 mm wide, 150 µm high and 5 mm long directly above the magnets, which is joined to a channel 500 µm wide, 150 µm high and 6.5 mm long that makes the solution pass over the electrodes. The microband gold electrodes consist of three bands 500 µm wide and one band 1 mm wide, all parallel and separated from each other by 100 µm gaps. The wider band was used as auxiliary electrode and the upstream-most microband was used as the pseudo-reference to avoid potential shifts during the measurements. The assay consists of the following steps: (1) Immunocapture of target bacteria with MP, labelling with HRP-Ab and injection in the microfluidic system. (2) Magnetic confinement of MP in the reaction chamber where enzyme reaction takes place. (3) Reduction of enzyme-produced BQ at the gold electrodes, downstream. The different biocomponents are not drawn to scale.

Figure 2. Optimisation of the sandwich immunoassay on MP. (a) Comparative performance of the two-step assay (■) and the 40-minute one-step approach (●). (b) Comparative performance of the one-step sandwich extended for 20 (▼), 40 (●), and 60 minutes (▲). (c) Specificity of the one-step sandwich assay for *E. coli* (■) versus *P. Putida* (●).

Figure 3: Detection of HRP using the flow cell. (a) Chronoamperograms obtained over time for increasing concentrations of HRP captured on MP(1 mM of H_2O_2 and 1 mM of HQ) (b) Calibration plot for the steady-state intensity current after 250 seconds of measurement.

Figure 4: Calibration plot of the steady-state current registered after 250 seconds of measurement for increasing bacterial concentrations. (Inset) Examples of the chronoamperograms obtained for the different bacterial concentrations.

Figure 5: Microfluidic detection in the absence (control) or in the presence of 100 *E. coli* cells ml^{-1} in either PBS or milk (10%). (Top) Values of the initial reduction peak (absolute values) and the steady state current obtained for 3 independent samples. (Bottom) Averaged peak currents. The inset shows an example of the chronoamperograms obtained in PBS (black line, negative control; grey line, *E. coli*). By convention, negative signs indicate a reduction current. SD stands for *standard deviation*.

Figure 1 - updated

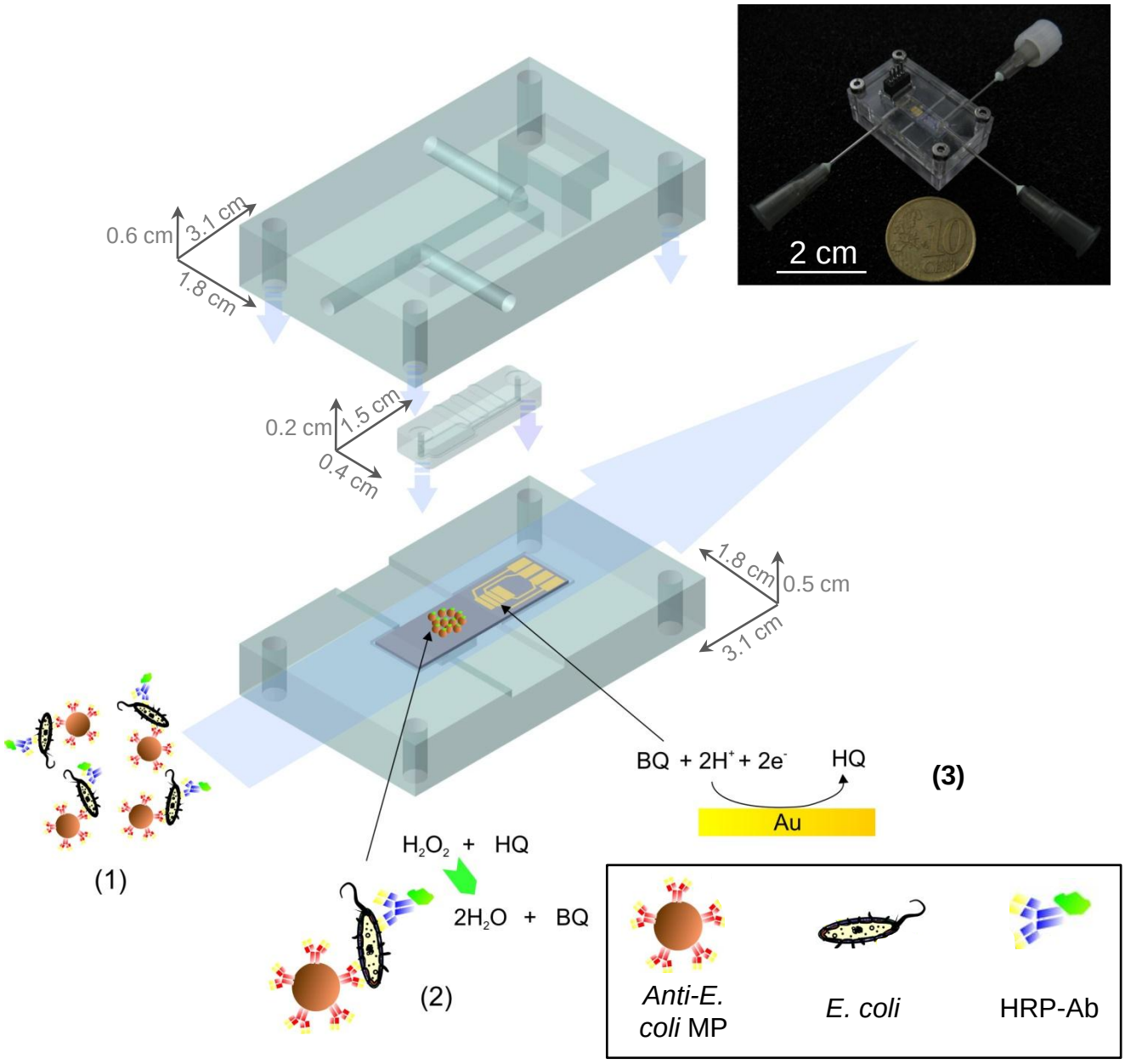

Figure 1

Figure(s)

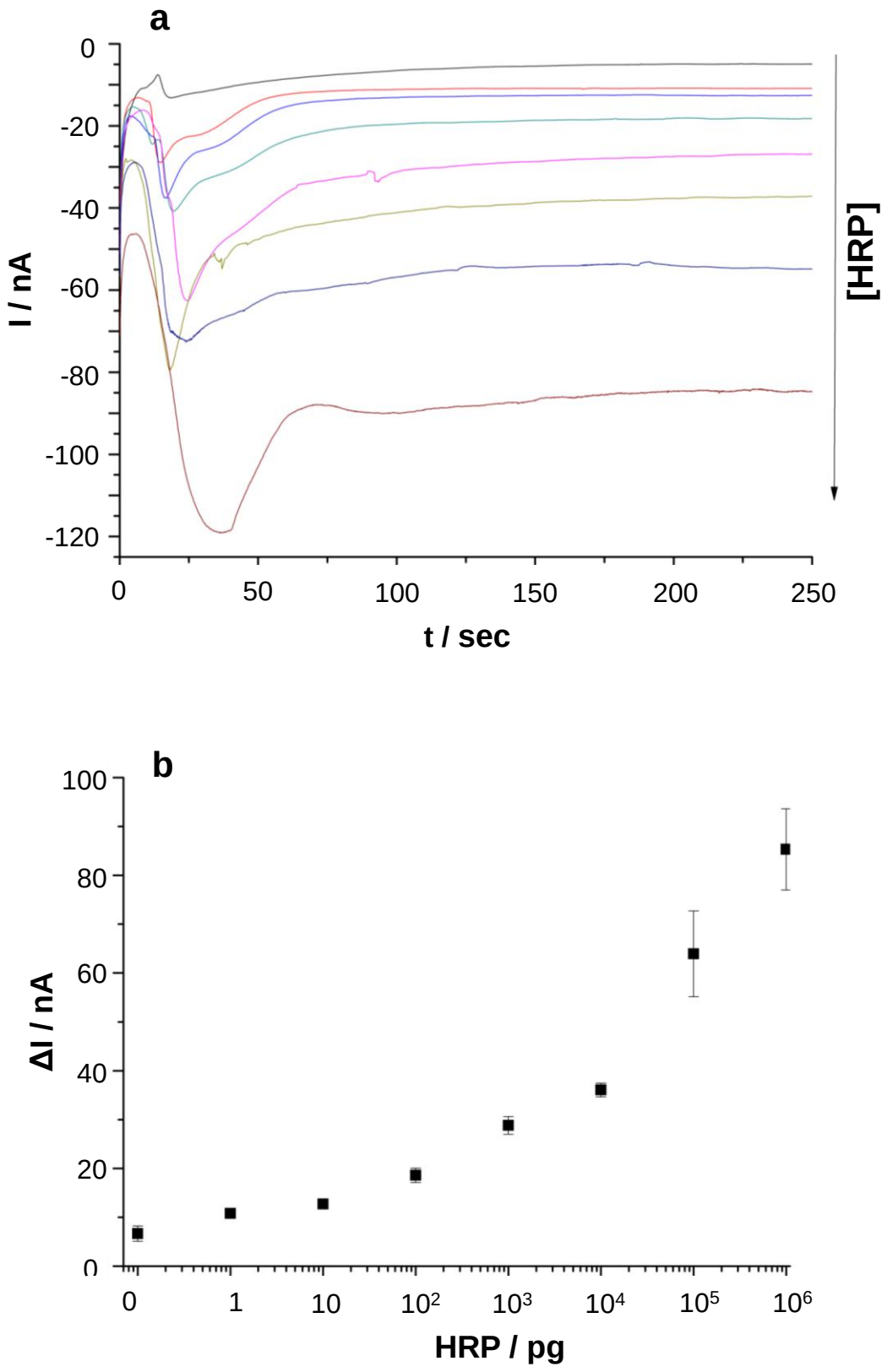

Figure 3

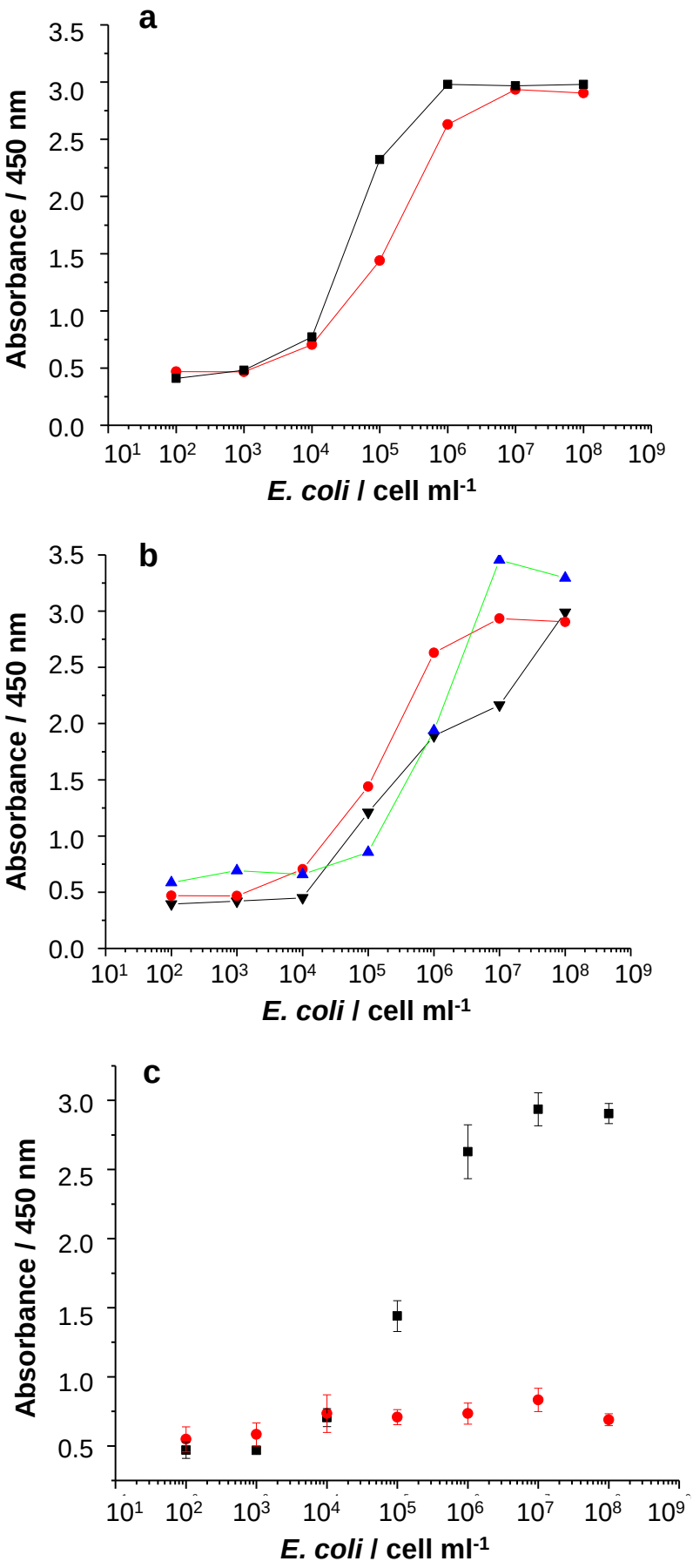
a
Absorbance / 450 nm
3.5
3.0
2.5
2.0
1.5
1.0
0.5
0.0
10¹ 10² 10³ 10⁴ 10⁵ 10⁶ 10⁷ 10⁸ 10⁹
E. coli / cell ml-1
b
Absorbance / 450 nm
3.5
3.0
2.5
2.0
1.5
1.0
0.5
0.0
10¹ 10² 10³ 10⁴ 10⁵ 10⁶ 10⁷ 10⁸ 10⁹
E. coli / cell ml-1
c
Absorbance / 450 nm
3.0
2.5
2.0
1.5
1.0
0.5
10¹ 10² 10³ 10⁴ 10⁵ 10⁶ 10⁷ 10⁸ 10⁹
E. coli / cell ml-1

Figure 2

Figure 4 - updated

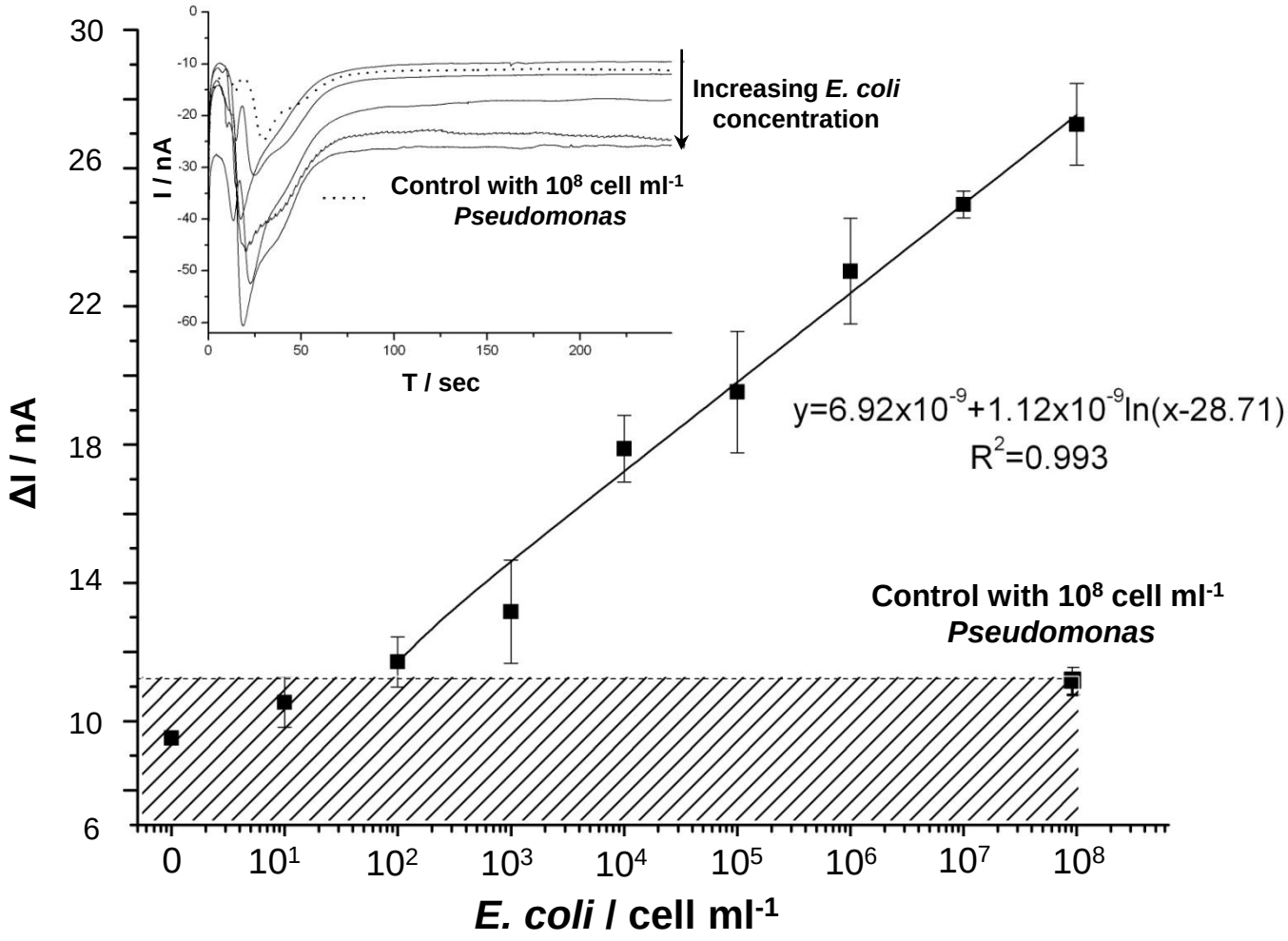

Figure 4

Figure(s)

		Sample	Peak height (nA)	Average	SD	Steady state current (nA)	Average	SD
PBS	Control	1	13.4	16.43	3.16	-19.3	-21.47	1.99
		2	16.2			-23.2		
		3	19.7			-21.9		
	100 *E. coli* ml^{-1}	1	24.2	26.80	2.31	-28.7	-27.37	1.46
		2	27.6			-25.8		
		3	28.6			-27.6		
Milk 10%	Control	1	5.7	6.90	1.51	-9.1	-8.27	0.91
		2	8.6			-8.4		
		3	6.4			-7.3		
	100 *E. coli* ml^{-1}	1	10.8	12.07	1.36	-11.9	-10.60	1.25
		2	11.9			-10.5		
		3	13.5			-9.4		

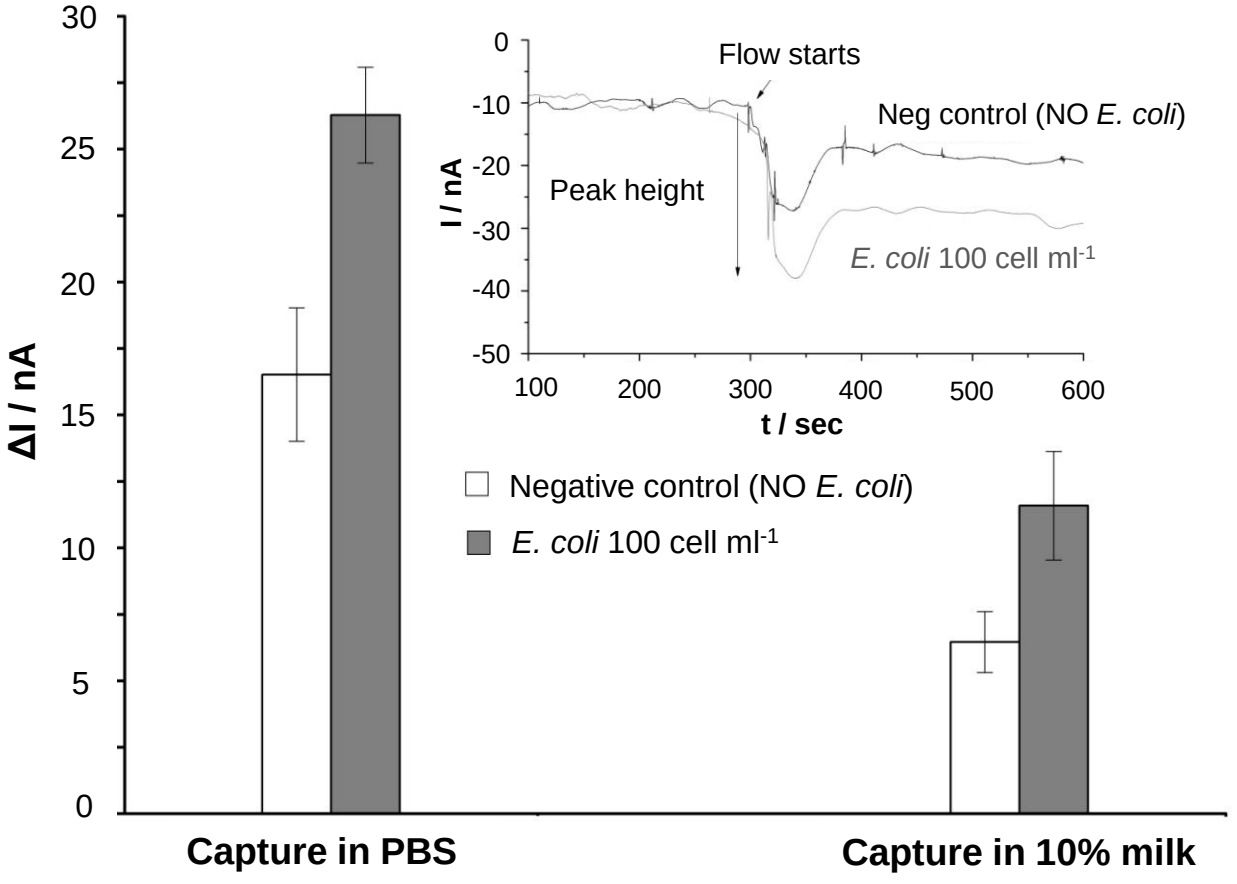

Figure 5